Modelling daily precipitation features in the Volta Basin of West Africa

P. Laux,[a]* S. Wagner,[a] A. Wagner,[a] J. Jacobeit,[b] A. Bárdossy[c] and H. Kunstmann[a]

[a] *Institute for Meteorology and Climate Research (IMK-IFU), Forschungszentrum Karlsruhe, 82467 Garmisch-Partenkirchen, Germany*

[b] *Institute for Geography, University of Augsburg, 86135 Augsburg, Germany*

[c] *Institute for Hydraulic Engineering, University of Stuttgart, 70569 Stuttgart, Germany*

ABSTRACT: The combination of a conventional Markov chain model (zero and first order) and a gamma distribution model are found to be applicable to derive meaningful agricultural features from precipitation in the Volta Basin (West Africa). Since the analysis of the monthly or annual precipitation amount does not provide any adequate information on rainfall timing and sufficiency of crop water requirement, rainfall modelling was performed on a daily time scale for 29 rainfall stations. The modelled rainfall features follow distinct spatial patterns, which will be presented as maps of(1) rainfall occurrence probabilities and (2) recommendations of optimal planting dates. In addition, the effective drought index (EDI) working on daily time scales is calculated in order to assess drought properties of five different rainfall regions within the Volta Basin. Apart from the common way of separately modelling the duration and intensity due to their different distributions, a copula approach is chosen in this study to construct a bivariate drought distribution. Application of the measures derived to agricultural decision support will be discussed briefly.

KEY WORDS agricultural planning; West Africa; Markov chain model; external drift kriging; onset of the rainy season; drought analysis; effective drought index (EDI); Clayton copula

1. Introduction

Spatial and temporal variations of crop yield may have profound impacts on humans and their environment (Pielke *et al*., 1998). This variability results from changes of numerous factors, in particular, physical and chemical soil properties, temperature, precipitation, solar radiation and human management. Of all climatic factors in tropical areas, precipitation variability is considered to be the most critical factor for rain-fed agriculture. Several studies have been carried out so far with respect to rainfall fluctuation in West and Central Africa (e.g. Le Barbé and Lebel, 1997; D'Amato *et al*., 1998; Mahé *et al*., 2001; L'Hôte *et al*., 2002; Neumann *et al*., 2007). Mahé *et al*. (2001) calculated standardized mean annual rainfall series for 23 countries of West and Central Africa. They used the regional vector method to derive 44 homogeneous climatic units and analysed them for discontinuities using different statistical tests. As a result, they identified a main discontinuity period between 1968 and 1970 followed by a second one at the beginning of the 1980s, with both periods being marked by severe drought events with greater rainfall deficits north of 10°N. The study of L'Hôte *et al*. (2002) confirmed the main discontinuity around 1970.

Footprints of climate change in the Volta Basin were reported by Neumann *et al*. (2007), revealing detailed trend analysis of the temperature-, precipitation- and discharge-time series observed. Kunstmann and Jung (2007) discussed the impact of intensifying agriculture due to population pressure and accompanying land use changes on rainfall.

In the drought−prone Sahelian countries, life is revolving around the occurrence or non-occurrence of rainfall and its temporal and spatial distribution (Sivakumar, 1992). Due to the limitation of precipitation to a few months per year (rainy season), adapted farming management strategies are of crucial importance to ensure sustainable food production. According to Sivakumar (1988), rainfall analysis is applied above all in crop and disaster planning, and the variable nature of rainfall is often given to be the main reason for the frequent crop failures and food shortages. Determination of the optimal planting time is a major concern. The amount of water available to plants strongly depends on the onset of the rainy season (ORS), length and termination (Ati *et al*., 2002). According to Steward (1991) and Ingram *et al*. (2002), the ORS is the most important variable. For sowing, it is important to know, whether (1) the rains are continuous and sufficient to ensure enough soil moisture

* Correspondence to: P. Laux, Institute for Meteorology and Climate Research (IMK-IFU), Forschungszentrum Karlsruhe, Kreuzeckbahnstraße 19, 82467 Garmisch-Partenkirchen, Germany.
E-mail: patrick.laux@imk.fzk.de

during planting and (2) whether this level will be maintained or even increased during the growing period to avoid crop failure (Walter, 1967). Knowledge of the ORS, cessation, and, hence, of the length of the rainy season is of great help in the timely preparation of farmland, mobilization of seed/crop, manpower and equipment and will also reduce the risk of planting and sowing too late or too early (Omotosho *et al*., 2000). Laux *et al*. (2008) developed a reliable regional, solely precipitation-based ORS definition as well as two different prediction methods for the ORS in the Volta Basin. An important criterion of this approach is the occurrence of a dry spell >6 days within the following 30 days in order to avoid total crop failure. Calculating these dry spell occurrence probabilities may therefore assist farmers in their decision on the sowing date. According to Sultan *et al*. (2005), who used a crop model for their study, large-scale climate variability influences crop yields mainly in terms of the choice of the sowing date, the annual rainfall totals and the intra-seasonal rainfall distribution. They identified the following intra-seasonal rainfall patterns by averaging rainfall in the region from 2.5 °W to 2.5 °E and 12.5 °N to 15°N, which are very consistent over the analysed period from 1968 to 1990:

- around 40 days with the largest amplitude during July and August;
- around 15 days with the largest amplitude in the first part of July and around the end of August to mid-September;
- around 3–6 days with the largest amplitude from the end of June, which is related to the onset of the rains, to the end of July, followed by a dry spell period centred in the beginning of August.

Le Barbé *et al*. (2002) characterized rainfall regimes over West Africa by analysing daily rainfall time series in terms of the average number of events over a given period of time and the average cumulative rainfall per event separated for the wet period 1951–1970 and the dry period 1971–1990. They found no spatially organized structure in the mean event rainfall, but well organized patterns in the mean number of events.

For agricultural impact studies, it is advisable to consider additional rainfall parameters like the probabilities of a day exceeding a certain threshold, the dry spell probabilities as well as the overall chance of rain (e.g. Usman and Reason, 2004). Determination of the number of wet days yielding specific amounts of rain is a necessary step to better understand the prevailing rainfall characteristics. The knowledge of heavy rainfalls with potential erosive impacts – e.g. precipitation rates >20 mm/day (e.g. Kowal and Kassam, 1978) - and their spatial distribution is of high relevance to agriculture. Not less important are the probabilities of dry spells at critical times during the growing season, especially at the beginning when they can hinder germination and during the establishment period.

Dry spells are directly related to agricultural impacts (e.g Sivakumar, 1992), since their frequency and duration indicate the degree of stress plants are exposed to. Additionally, an analysis of dry spells may indicate spatial differences in the rainfall consistency, thereby providing an assessment of the occurrence of rain-producing systems (Usman and Reason, 2004). The phenomenon of the decline in frequency and amount of daily rainfall for a number of weeks half way through the rainy season is called little dry season (LDS), leading to a bimodal rainfall regime in the southern part of the Volta Basin (Laux *et al*., 2008). The LDS is a consequence of the seasonal movement of the intertropical convergence zone (ITCZ). It may adversely affect the yields of early crops, if it takes place at the time of seed or tuber development. It may also delay planting of late crops. On the other hand, it provides e.g. favourable conditions for weeding, spraying insecticides and pesticides, and favours a good yield of yam. Deriving its spatially and temporally resolved occurrence probabilities would support the farmer's decision on scheduling seeding, weeding, harvesting, and the choice of the fruit. Furthermore, it is of major importance to know how long a wet spell/dry spell is likely to persist.

Since the economy of the Volta Basin is strongly depending on rain-fed agriculture and hydro-power generation, droughts are creating a huge risk. Although it is not possible to avoid droughts, drought preparedness can be developed and their impacts can be managed (Smakhtin and Hughes, 2007). The enhanced risk connected with droughts, in turn, discourages investment by farmers, governments and development agencies (Shapiro *et al*., 2007). Realistic and reasonable drought prediction requires a comprehensive understanding of the past drought variability.

A precise definition of a drought is an essential prerequisite to assess drought variability. Current definitions of drought vary from region to region and may depend on the predominating perception and the task for which it is defined. The only common feature is that every drought event effectively results from the lack of precipitation (Wilhite and Glantz, 1985) and therefore is a meteorological drought at first. Depending on its duration, a meteorological drought may result in an agricultural or a hydrological drought. The concept of the agricultural drought is linked with the lack of available water and agricultural impacts. In turn, the crop water requirement depends on local weather conditions, soil and plants' characteristics, and the plant's stage of growth. An agricultural drought should therefore be ideally defined in terms of its impact on a specific plant on a specific soil in a specific area, which makes it difficult to determine. Due to the absence of this agriculturally relevant information for the Volta Basin, drought analysis has been performed on the basis of daily rainfall data exclusively.

As droughts are regional by nature and commonly cover large areas, it is important to study such events within a regional context (Hisdal and Tallaksen, 2003). Therefore, the Volta Basin was divided into a manageable number of areas showing similar rainfall characteristics

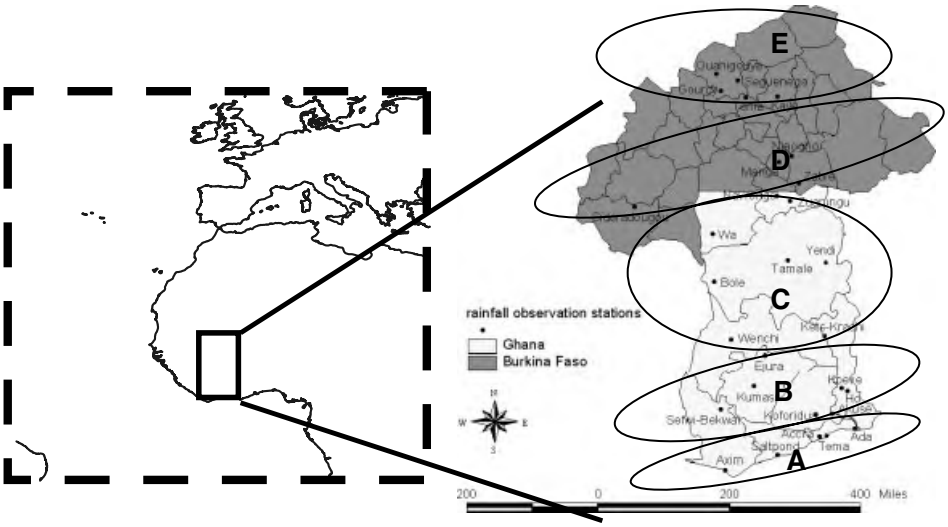

Figure 1. Location of the Volta Basin and spatial distribution of areas with similar rainfall characteristics, represented by five ellipses (right), (source: Laux *et al*., 2007).

prior to the drought analysis, following the approach of Laux *et al*. (2008). Figure 1 illustrates the location of the rainfall gauges as well as the five different rainfall regions represented by five ellipses.

In order to compare the strengths of droughts in different regions, regardless of their climatic differences, several standardized indices have been developed. Morid *et al*. (2006) compared different drought measures for drought monitoring in the Tehran province of Iran. The standardized precipitation index (SPI) and the effective drought index (EDI) were found to be suitable for consistently detecting the onset of a drought and its spatial and temporal variation. Therefore, they were recommended for operational drought monitoring. The EDI was found to be more sensitive to the emerging drought than the SPI (Morid *et al*., 2006).

As droughts may be considered stochastic processes, stochastic modelling is a proper approach to assess their characteristics (Shiau *et al*., 2007). Many research papers deal with a univariate analysis of droughts (e.g. Dracup *et al*., 1980a,b; Mathier *et al*., 1992; Cancelliere and Salas, 2004). However, univariate analysis cannot simultaneously account for the correlation of drought duration and drought intensity (Shiau *et al*., 2007). For this reason, a bivariate distribution, which jointly describes these two aspects was adopted. For the bivariate or multivariate analysis of two or more variables with unknown or different distribution, Copula functions can be used.

The purpose of this paper is twofold: (1) due to the above-mentioned importance of the analysis of rainfall on an intra-seasonal time scale, the main objective of this paper is to derive agricultural meaningful rainfall characteristics in the Volta Basin. As an example, the overall rainfall probabilities and dry spell probabilities are calculated on the plot scale and regionalized via kriging algorithms in order to generate risk maps for agriculture in the Volta Basin; (2) the second aspect deals with stochastic drought modelling on the regional scale using the EDI. Combining drought intensity and drought duration by means of a Clayton copula function allows for a more realistic classification of droughts in terms of risks and return intervals. Using the EDI for drought definition provides an objective tool for drought monitoring in the Volta Basin.

2. Data set

Totally, 29 observation time series of the Volta Basin with daily resolution were used for the statistical analyses. The meteorological data were obtained from the Institut National de l'Environnement et des Recherches Agricoles (INERA) at Ouagadougou (Burkina Faso), the Meteorological Service of Burkina Faso in Ouagadougou and the Meteorological Service Department in Accra (Ghana). The data had been checked for continuity and plausibility by the two services. Due to large data gaps in most of the observation time series, only a limited number of the meteorological observation stations could be used.

3. Methodology

3.1. Deriving relevant rainfall features

Generalized linear models are used by numerous researchers for modelling rainfall. Often, two models are considered separately, one for rainfall occurrence and the other for rainfall amounts. The former is often modelled using a binomial distribution and the latter by a gamma distribution (e. g. Stern and Coe, 1982). Dunn and White (2005) even proposed an integrated approach using the power-variance exponential dispersion models. For the work described here, two models were used, a Markov model for rainfall occurrence and a gamma distribution for modelling the rainfall amounts. Besides unconditional probability (zero-order Markov chain), the simplest solution for modelling rainfall occurrence is a two-state (occurrence of precipitation or not) first-order

(precipitation probability depends solely on the previous day's precipitation occurrence) Markov model, which can be defined by two transition probabilities:

$$P_{01} = P \text{ (rainfall on day } t \mid \text{no rainfall on day } t-1) \quad (1)$$

and:

$$P_{11} = P \text{ (rainfall on day } t \mid \text{rainfall on day } t-1) \quad (2)$$

The two complementary transition probabilities are $P_{00} = 1 - P_{01}$ and $P_{10} = 1 - P_{11}$. Generally, high-order Markov chain models are also used to model sequences of rainy or dry spells (Chin, 1977). For a two-state Markov model, the number increases exponentially with the order of the process, in general, 2^k for kth order. As described by Stern *et al.* (1981), the observed proportions, P, are transformed using the logit transformation:

$$f = \log\left(\frac{P}{1-P}\right) \quad (3)$$

This allows f to vary from $-\infty$ ($P = 0$) to $+\infty$ ($P = 1$). Former studies showed that Fourier series are particularly suited to fit both unimodal and bimodal seasonal patterns, with the advantage that the fitted probabilities at the start and the end of the year are equal (Garbutt *et al.*, 1981). On the other hand, Fourier series can be used for smoothing inherently noisy parameter sets (Jimoh and Webster, 1999). The fitted probabilities are given by:

$$y = \frac{\exp^f}{(1+\exp^f)}, \quad (4)$$

where f is the sum of the Fourier series:

$$f = a_0 + \sum_{j=1}^{n}(a_j \cos jt + b_j \sin jt), \quad (5)$$

where $t = \pi$ (date – 183)/183 and n is the number of harmonics. In our study, the number of harmonics was set to 4.

The distribution of daily rainfall amounts is highly skewed. Gamma distribution is regarded to be most appropriate to model daily rainfall volumes (Buishand, 1977). Since the mean rain per year often varies throughout the year, it is useful to consider models which reflect this temporal dependence (Stern and Coe, 1982). Gamma distributions were fitted to rainfall amounts of rainy days. Days with rainfall below a certain threshold were excluded. The gamma distribution is given by (e.g. Stern and Coe, 1982):

$$f(x) = \left(\frac{K}{\mu}\right)^K \frac{(x-c)^{K-1}\exp^{-K(x-c)/\mu}}{\Gamma(k)}, \quad (6)$$

$\Gamma(k)$ is the gamma function with its shape parameter K and mean μ. Since these two parameters may vary temporally (i.e. within the season) and spatially (from site to site), their monthly values were estimated for each site. The rainfall amounts, x, are shifted by the threshold value c. In this study, rainfall thresholds from 0.5 to 2.0 mm with an increment of 0.5 mm were used and compared. The results differ scarcely (not shown within this paper). Therefore, a mean threshold of 1 mm was assumed in the following calculations. The Famine and Early Warning System (FEWS) of the United States Agency for International Development uses 0.85 mm of rain as the minimum value for a wet day. In addition, occurrence probabilities of a dry spell of 6 or more consecutive days within the following 30 days were calculated for each day of the year (DOY). The dates of the minimum probabilities as well as their probabilities were spatially interpolated by external drift kriging.

Kriging is a geostatistical method that uses the variogram of the regionalized variable (i.e. the variance between pairs of points that lie different distances apart) to estimate interpolated values. The 'best' estimate of the values (BLUE: Best Linear Unbiased Estimator) is calculated, taking into account the layout of the observation network relative to the interpolation grid. The external drift kriging method (Ahmed and de Marsily, 1987) additionally incorporates external knowledge in the system as external drift. Here, it is supposed that an additional variable exists that is linearly related to the regionalized variable. The estimator thus depends on the additional variable, which therefore has to be available at a high spatial resolution, preferably as a regular grid. In contrast to ordinary Kriging, the expected value of the regionalized variable is not constant, but linearly related to the one or more additional variables.

In West Africa, the structure of rain fields is dominated by two major factors that have to be considered for spatial interpolation (e.g. Ali *et al.*, 2003): First, the displacement of convective systems in the privileged east–west direction, and second, a decreasing south–north gradient of mean annual rainfall due to the seasonal migration of the ITCZ. Both factors yield to higher correlations of observations in east–west than in north–south direction and hence to a latitudinal dependence of the spatial precipitation distribution. This effect is taken into account in the simulations by applying an anisotropy factor and using the distance-to-sea information for each grid point as external drift.

For this study, experimental variograms were calculated for the mean μ and shape parameter K of the gamma distribution and monthly rainfall occurrence probabilities exceeding 5 and 20 mm/day. The results of the variogram analysis – nugget and sill and range of exponential model – are summarized in Table I. The variogram parameters for the interpolation of the mean μ and shape parameter K of the Gamma distribution show that the microscale variation which is given by the nugget value is minor compared to the total variation. But for the rainfall occurrence probabilities, the mean microscale variation describes 55% for 5 mm and 72% for 20 mm of the total ones. Furthermore, the seasonal variations are

Table I. Variogram analysis of optimal planting time and probability, mean μ and shape parameter K of the gamma distribution, and monthly rainfall occurrence probabilities exceeding 5 and 20 mm/day.

	Nugget	Sill	Range [km]
Optimal planting time	16.43	246.11	240
Optimal. planting prob.	13.50	78.65	250
μ	0.01	0.83	250
K	0.00	0.25	110

	Nugget	Sill	Range [km]
5 mm: mean	66.13	119.03	240
5 mm: std	50.85	87.42	70.11
20 mm: mean	19.92	27.72	240
20 mm: std	13.54	11.55	95.43

high which leads to high standard deviation values for all variogram parameters.

Figure 2 illustrates the long-term mean annual rainfall (1961–1999) using ordinary kriging and external drift kriging with distance-to-sea information as spatial interpolation methods. External drift kriging exhibits more realistic patterns in areas with a patchy and low-density meteorological observation network. The patterns and values of the precipitation interpolation by external drift kriging are in good agreement with the results of ORSTOM (1996). In further analyses of this study, external drift kriging will therefore be applied for the spatial interpolation of rainfall-related properties.

3.2. Drought definition

Drought indices are well suited to quantitatively assess drought properties. In this study, a drought is defined as a period with negative effective EDI values and drought duration and drought intensity are derived from the EDI: The first step is the calculation of daily effective precipitation (EP)), which is defined as a function of precipitation of the current day and precipitation of the previous days – with lower weights. The duration of the preceding period, over which the EP amount is calculated, may vary. For this study, the EP was calculated over 365 days.

$$EP_j = \sum_{n=1}^{i}[(\sum_{m=1}^{n} P_m)/n], \tag{7}$$

where j is the index of a current day, i is the duration over which the sum is calculated, and P_m is the precipitation $m-1$ days before the current day. For example, if i equals 3, then the EP equals $[P_1 + (P_1 + P_2)/2 + (P_1 + P_2 + P_3)/3]$. The next step includes the calculation of the mean EP for each day of the year, the MEP_j. This is followed by the calculation of daily deviations of EP from MEP, the DEP, the standard deviations (ST(EP)) for each calendar day and the standardized value of daily deviations SEP, which allows drought intensity at two or more locations to be compared with each other regardless of climatic differences between them.

$$\text{SEP} = \text{DEP}/\text{ST(EP)} \tag{8}$$

Drought duration may now be defined similarly to e.g. the SPI as a period where SEP is consistently negative. After the calculation of daily *DEP* values, it is possible to compute the precipitation needed for a return to normal conditions (PRN). By description, PRN is precipitation necessary to recover from the accumulated deficit. Daily *PRN* values, however, should take into account the actual

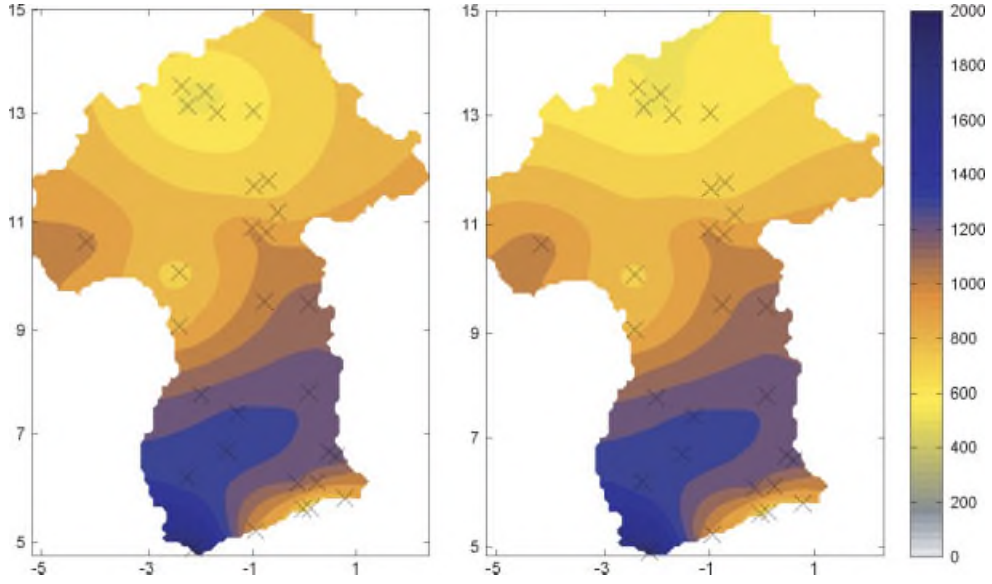

Figure 2. Spatial interpolation of the annual rainfall amount (mm) using ordinary kriging (left) and external drift kriging with the distance-to-sea (right). Observation data from 1961 to 1999 of 29 synoptic stations (represented by crosses) were used for interpolation.

duration over which *DEP* values have been calculated:

$$\mathrm{PRN}_j = \frac{\mathrm{DEP}_j}{\sum_{N=1}^{j}(1/N)} \tag{9}$$

where j is actual duration. Finally, the EDI is calculated as the standardized value of PRN:

$$\mathrm{EDI}_j = \frac{\mathrm{PRN}_j}{ST(PRN_j)} \tag{10}$$

where ST(PRN)is the standard deviation of each day's PRN.

From the EDI, quantitative drought characteristics, such as the onset, cessation, duration D, intensity S, and inter-arrival time τ (time between the onsets of two consecutive droughts), can be derived objectively. A meteorological drought is defined as a period of time in which the calculated EDI is negative (Figure 3). A change of sign from positive values to negative values defines the onset and, vice versa, the cessation of a drought. The integral of the absolute values of the EDI between onset and cessation of a drought is a measure of the drought intensity. Before applying this definition to the EDI time series, a moving-average filter of different window sizes is applied to prevent a very short, but heavy shower event from being misinterpreted as the end of the drought. The application of a moving-average filter is recommended to pool mutually dependent negative meteorological droughts (e.g. Tallaksen *et al.*, 1997). A moving-window of 10 days was chosen to assess reasonable drought properties in terms of a more agriculturally rather than meteorologically oriented drought definition. Working with unfiltered EDI values would skew the distribution of the derived statistical drought measures. However, short showers after long dry spell may have profound negative impacts on agriculture in terms of soil erosion (e.g. Chatterjea, 1998). In turn, short showers can also be seen as a benefit, because they can sustain the vegetative cycle for some more days and thus ensuring the survival of the crops, especially in the Sahelian zone. For sake of simplicity, no differentiation of the drought definition between the different agro-ecological zones within the basin was applied. A moving-average filter of 10 days is found capable to exclude most of these short intermittent events, but simultaneously keeps the original structure of the EDI time series.

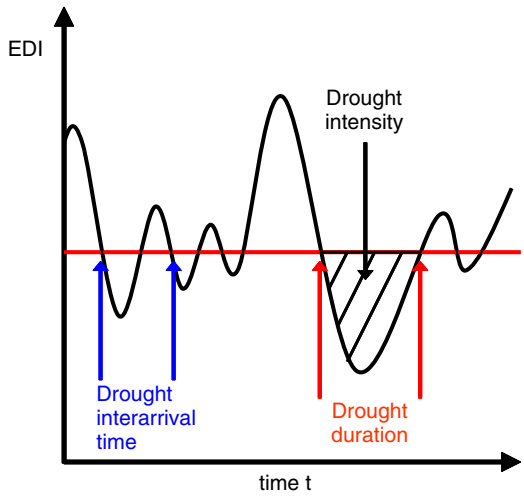

Figure 3. Schematic illustration of calculation of drought-specific parameters based on the effective drought index (EDI). This figure is available in colour online at www.interscience.wiley.com/ijoc

3.2.1. *Copula-based approach*

Copulas were first mentioned in literature by Sklar (1959) and are nowadays widely used for financial or insurance applications. The basic idea behind this approach is to separate the dependence and the marginal distributions in a multivariate distribution. Sklar's theorem states that if H is a joint distribution function of d random variables with $F_1, \ldots, F_d$ marginal distribution functions, then a copula C exists, such that:

$$H(x_1, \ldots, x_d) = C[F_1(x_1), \ldots, F_d(x_d)] \tag{11}$$

Conversely, if C is a copula and $F_1, \ldots, F_d$ are distribution functions, H is a joint distribution function with marginal distribution functions $F_1, \ldots, F_d$. In other words, a copula describes how the marginals are tied together. Another practical aspect of copulas is that they are not limited to any distinct distribution of the random variables, in contrast to the Bravais Pearson correlation coefficient r_{bp} which is restricted to the (multivariate) normal distribution. Other dependence measures like the Spearman rank correlation coefficient ρ_s or Kendall's Tau τ_k just express the 'average dependence' in the form of one single value.

Clayton's copula has already been proved suitable to construct the bivariate distribution of drought duration (D) and drought intensity (S) (Shiau *et al.*, 2007). For this reason, it was applied in this study as well. The Clayton copula (Equation (12)) and its density function (Equation (13)) are of the form:

$$C(u, v) = (u^{-\Theta} + v^{-\Theta} - 1)^{-1/\Theta}, \ \Theta \geq 0 \tag{12}$$

$$c(u, v) = (\Theta + 1)(u^{-\Theta} + v^{-\Theta} - 1)^{-(1/\Theta)-2} (uv)^{-\Theta-1} \tag{13}$$

The parameter Θ is a measure of the degree of association between u and v. There is no loss of generality working on unit square (u, v) instead of the original variable space (d, s), because u and v can be transformed back again, using:

$$u = F_D(d) \Leftrightarrow d = F_D{}^{(-1)}(u) \tag{14}$$

$$v = F_S(s) \Leftrightarrow s = F_S{}^{(-1)}(v) \tag{15}$$

The Clayton copula parameter Θ from Equations (12) and (13) can either be estimated from the data by means

Table II. Mean drought duration [days], mean drought intensity [cum. EDI values], mean interarrival time [days], and degree of association between drought duration and drought intensity Θ of the five different rainfall regions within the Volta Basin using a 10-day moving-average filter for the EDI values.

Rainfall region	Mean drought duration	Mean drought intensity	Mean inter-arrival time	Θ
A	86.02	70.90	170.16	5.78
B	116.39	84.16	204.23	7.29
C	72.42	57.50	147.77	10.11
D	94.79	74.60	186.94	7.50
E	77.62	56.21	143.65	5.51

of Kendall's Tau τ_k or it can be estimated numerically using e.g. Newton's method. Here, the second method is applied. The likelihood function of the copula is maximized to obtain the estimate $\hat{\Theta}$ of the copula parameter Θ. The values of $\hat{\Theta}$ can be found in Table II. The drought distribution for region B based on Clayton's copula can therefore be expressed as:

$$F_{D,S}(d,s) = C[F_D(d), F_S(s)] = [(F_D(d)^{-7.29} + F_S(s)^{-7.29} - 1)]^{-1/7.29} \quad (16)$$

3.2.2. *Drought return intervals*

The return period is a simple, but efficient criterion for risk analysis (Salvadori, 2004). It is usually defined as the average time elapsing between two successive occurrences of an event. The analysis of return periods is often limited to univariate cases, e.g. the return periods τ of drought duration (index D) and drought intensity (index S) can be defined separately as:

$$\tau_D = \frac{\overline{L}}{1 - F_D(d)} \quad (17)$$

$$\tau_S = \frac{\overline{L}}{1 - F_S(s)} \quad (18)$$

where $\overline{L}$ denotes the mean inter-arrival time of droughts (Figure 3) and F denotes the cumulative density functions (CDF) of drought duration and drought intensity.

Since natural events are often characterized by the joint behaviour of several non-independent random variables, this may lead to an over- or underestimation of the risk of the event. Consequently, the event should be defined in terms of two or more variables (Salvadori *et al.*, 2004). Instead of considering a particular joint distribution F_{XY} with well-specified marginals F_X and F_Y, bivariate return periods were calculated using the copula approach. Two cases of bivariate drought periods can be defined by either drought duration and drought intensity exceeding a specific value ($\wedge$ - case) or by drought duration or drought intensity exceeding a specific value ($\vee$ case). Both cases can be calculated by:

$$\tau_{DS\_\vee} = \frac{\overline{L}}{1 - C[F_D(d), F_S(s)]} \quad (19)$$

$$\tau_{DS\_\wedge} = \frac{\overline{L}}{1 - F_D(d) - F_S(s) + C[F_D(d), F_S(s)]} \quad (20)$$

This methodology offers considerable advantages compared to the above approaches, because it will consider the joint distributions for all the marginals, and it is even possible to derive the analytical expressions of the isolines of the return periods (Salvadori *et al.*, 2007).

4. Results

Temporal distribution of rainfall was first investigated by analysing its overall probability. The probability of rainfall depends on the conditions of previous days (conditional probabilities). Before analysing the conditional probabilities, it is reasonable to determine the overall chance of rainfall (unconditional probability). By way of example, Figure 4 presents the observed and fitted rainfall probabilities (zero-order Markov model) at Accra based on rainfall data (1961–1999) with a threshold of 1 mm for a rainy day. The probability increases rapidly around DOY 100 (08/09 April), reaching a maximum of more than 50% during the first (major) rainy season from DOY 160 to 170 (08–18 June), remaining relatively constant at 25% from DOY 200 to 270 (18 July–26 September) during the second (minor) rainy season in this region, and decreasing again towards the end of the year. The overall chance of rain during the major rainy season is approximately twice the rainfall probability during the minor rainy season. During the months of January, February, November and December, the rainfall probability is less than 10%. Figure 5 shows the first-order Markov chain dealing with rainfall probability depending on whether the previous day was wet or dry. When

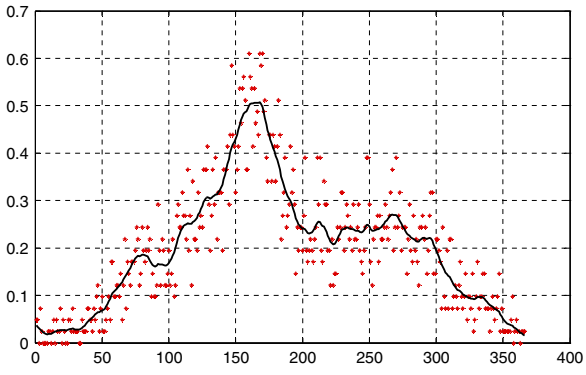

Figure 4. Overall rainfall probability (zero-order Markov model) for each day of the year at Accra, based on rainfall data (1961–1999) with a threshold of 1 mm for a rainy day, observed (*) and fitted (−) using Fourier series with four harmonics. This figure is available in colour online at www.interscience.wiley.com/ijoc

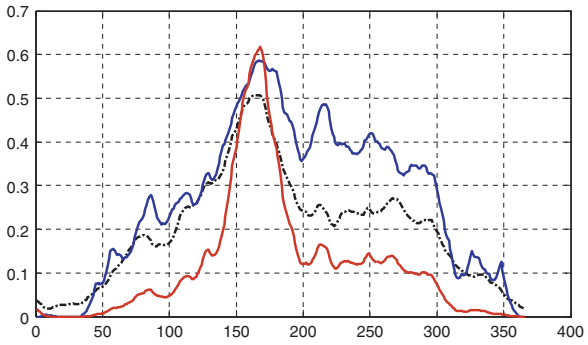

Figure 5. First-order Markov chain of Accra, the black line is the fitted line of the overall chance of rain. The red line stands for the probability of rain, if it is followed by a dry day (fitted), and the blue line stands for the probability of rain, if it is followed by a wet day (fitted).

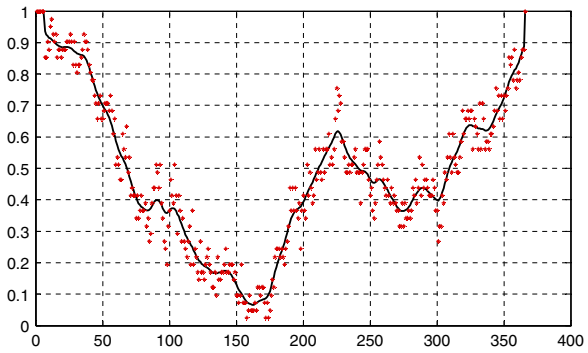

Figure 6. Observed (*) and fitted (−) dry spell occurrence probability within the following 30 days for each day of the year at Bole, based on rainfall data from 1961 to 1999. This figure is available in colour online at www.interscience.wiley.com/ijoc

comparing the conditional probabilities with the overall chance of rainfall (black line), it is found that the probability of rain following a rainy day is higher. For the time around the minor season (from DOY 200 until 300), the probability is about three times higher. In the period around the normal ORS in Accra (∼ day 85), a peak occurs, with the probability being more than twice as high as that of rain following a dry day. The overall chance of rainfall at a location predominantly ranges between the curves of rain following a rainy day and rain following a dry day.

Figure 6 exhibits the observed and fitted dry spell occurrence probabilities within the following 30 days calculated for each DOY at Bole. The probability decreases below 10% around DOY 160 (08 June). After this, the probability of dry spells increases to more than 60% (around 12 August). Then, it decreases again to less than 40% (25 September), and finally, it increases again rapidly. Assuming e.g. a probability threshold value of $P = 0.2$, which is not allowed to be exceeded at planting time, the time window for planting is restricted to the period from approximately DOY 120 to 180. These probabilities were calculated for all stations in the Volta Basin, and Figure 7 illustrates the spatial distribution of

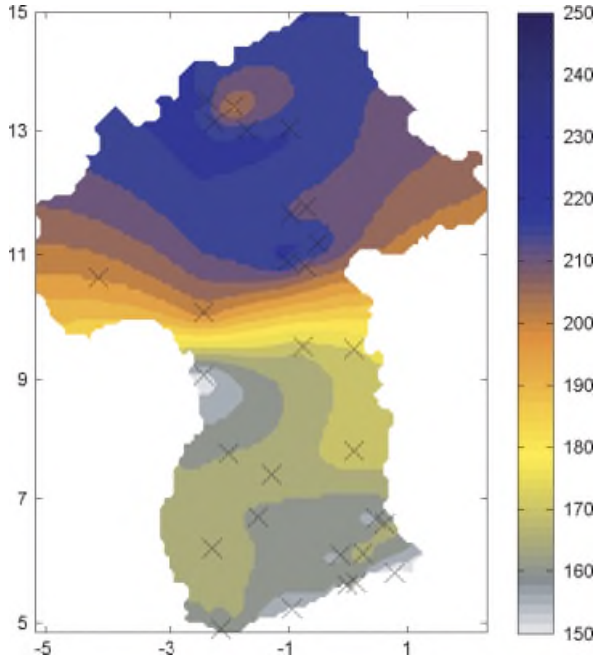

Figure 7. Date with minimum dry spell occurrence probability for the following 30 days, representing the optimal planting date (day of year). External drift kriging, including distance-to-sea information, was applied for spatial interpolation.

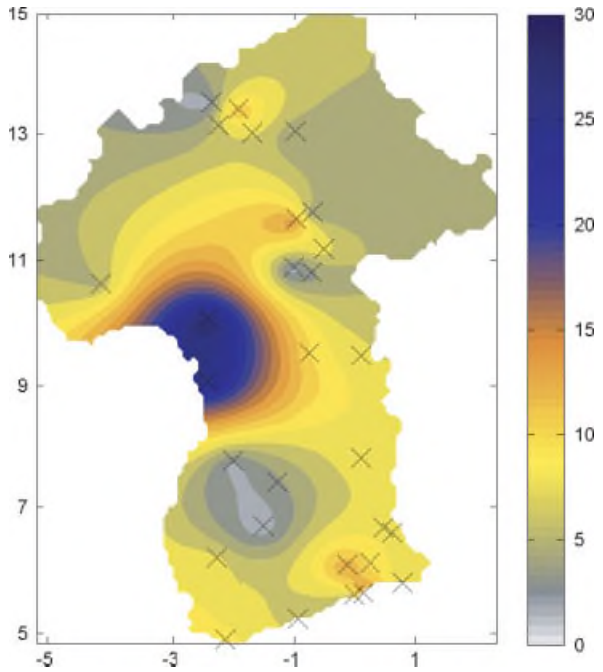

Figure 8. Probability of the dry spell occurrence within the following 30 days (%). External drift kriging, including distance-to-sea information, was applied for spatial interpolation.

the dates with minimum dry spell occurrence probabilities. Except for the stations Bole and Ejura (Figure 1), the pattern approximately reflects a north–south distribution following the movement of the ITCZ. The respective probabilities of these dates are presented in Figure 8. The minimum dry spell probabilities hold a regional maximum in the northwest of Ghana and southwest of Burkina

Faso (∼30%). This is of crucial importance to farming management. In these regions, dry spells are more likely to occur within the following 30 days and, thus, crop failure is more likely to occur. Focussed irrigation strategies especially in regions with a very high dry spell probability would be beneficial to enhance food security.

When modelling rainfall or dry spell probabilities, conditional probabilities should be considered to allow conclusions to be drawn with respect to their persistence in time. The transition probabilities help to estimate the reasonable order of the Markov chains. The first-order transition probabilities were found to be adequate for rainfall in the Volta Basin. Similar conclusions were drawn for rainfall in Nigeria (Jimoh and Webster, 1999).

The rainfall amount can be described adequately using a gamma distribution. Figure 9 depicts the modelled mean precipitation per rainy day at Accra for the wet period 1961–1969, the dry period 1970–1990 and the whole period 1961–1999 separately. Le Barbé *et al.* (2002) compare rainfall characteristics of the wet 1950–1969 period and the dry 1970–1990 period across West Africa. For some regions, they identified significant differences. Within this study, no significant changes of the seasonal cycles can be found comparing dry and wet periods, but remarkable differences in the rainfall amounts are detected. For station Accra, the highest differences occur during the major rainy season in June. The rainfall maximum for 1961–1999 is slightly higher than 8 mm and reached around June 8, followed by a period with less than 1 mm per day from DOY 195 to 260 and slightly larger than 2 mm/day up to DOY 300, and again smaller values to the end of year.

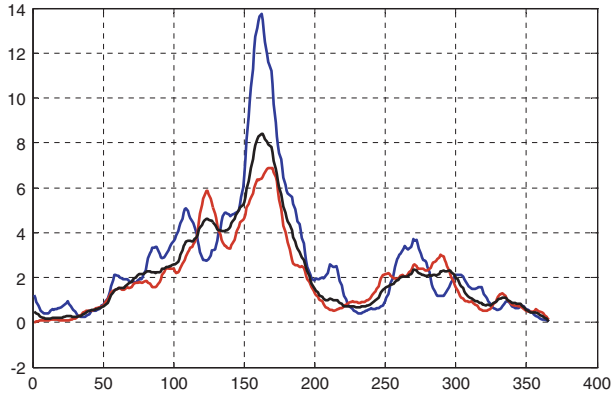

Figure 9. Fitted mean rainfall amount (mm) per day of year at Accra for the wet period 1961–1969 (blue line), the dry period 1970–1990 (red line) and the period 1961–1999 (black line). A Fourier series with four harmonics was used.

Figure 10 illustrates the mean spatial distribution of the mean μ and shape parameter K of the gamma distribution. Both parameters show a large spatial variability, which has to be taken into account for modelling the rainfall amounts. The observed patterns of μ, impacted mainly by the mean rainfall amount per day, and K, impacted mainly by the occurrence frequency of rainfall events of different magnitude, are generally arranged zonally and follow the climatological conditions in the Volta Basin. The highest values of the mean parameters K ($K \approx 5$) are found in the southwest of the Volta Basin where rainfall amounts up to 2000 mm per year (Figure 2). More northward, between latitudes of 6 and 7°N, the lowest values of K ($K \approx 1.5$) are observed. From 8 to 15°N, the values of K are increasing again to values of $K \approx 4$. The shape parameter μ is increasing rapidly from the coastal zone ($\mu \approx 1$) to 8°N ($\mu \approx 2.5$), and decreasing slowly to 15°N ($\mu \approx 0.3$). In the coastal zone of the basin, the shape parameter K is approximately 1. The distributions of three observation stations with different parameter combinations (Figure 11) are highlighted as follows.

According to the highest rainfall amounts in southwest Ghana, represented by station Axim (Figure 11, top), the

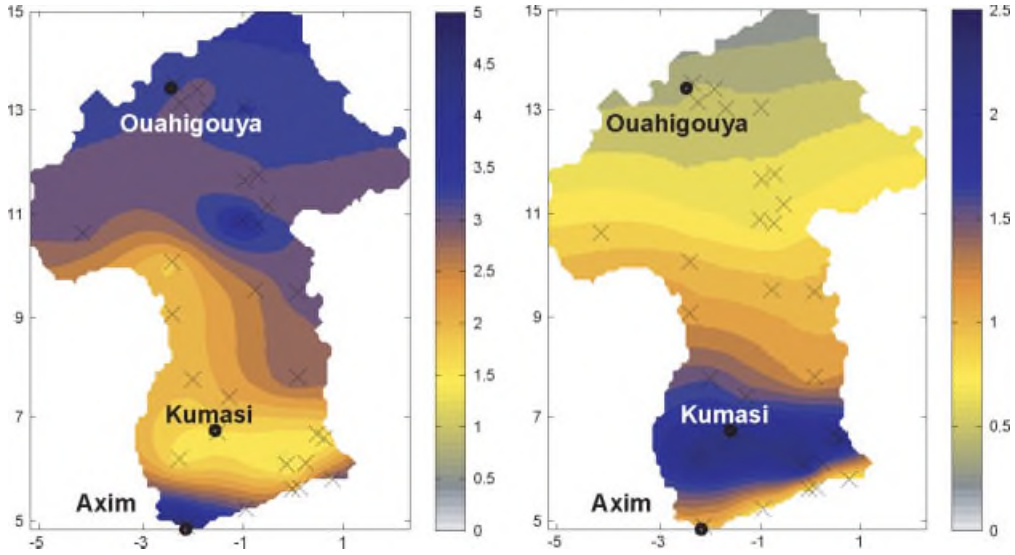

Figure 10. Spatial distribution of the mean μ (left) and the shape parameter k (right) of the gamma distribution, interpolated using external drift kriging with distance-to-sea information.

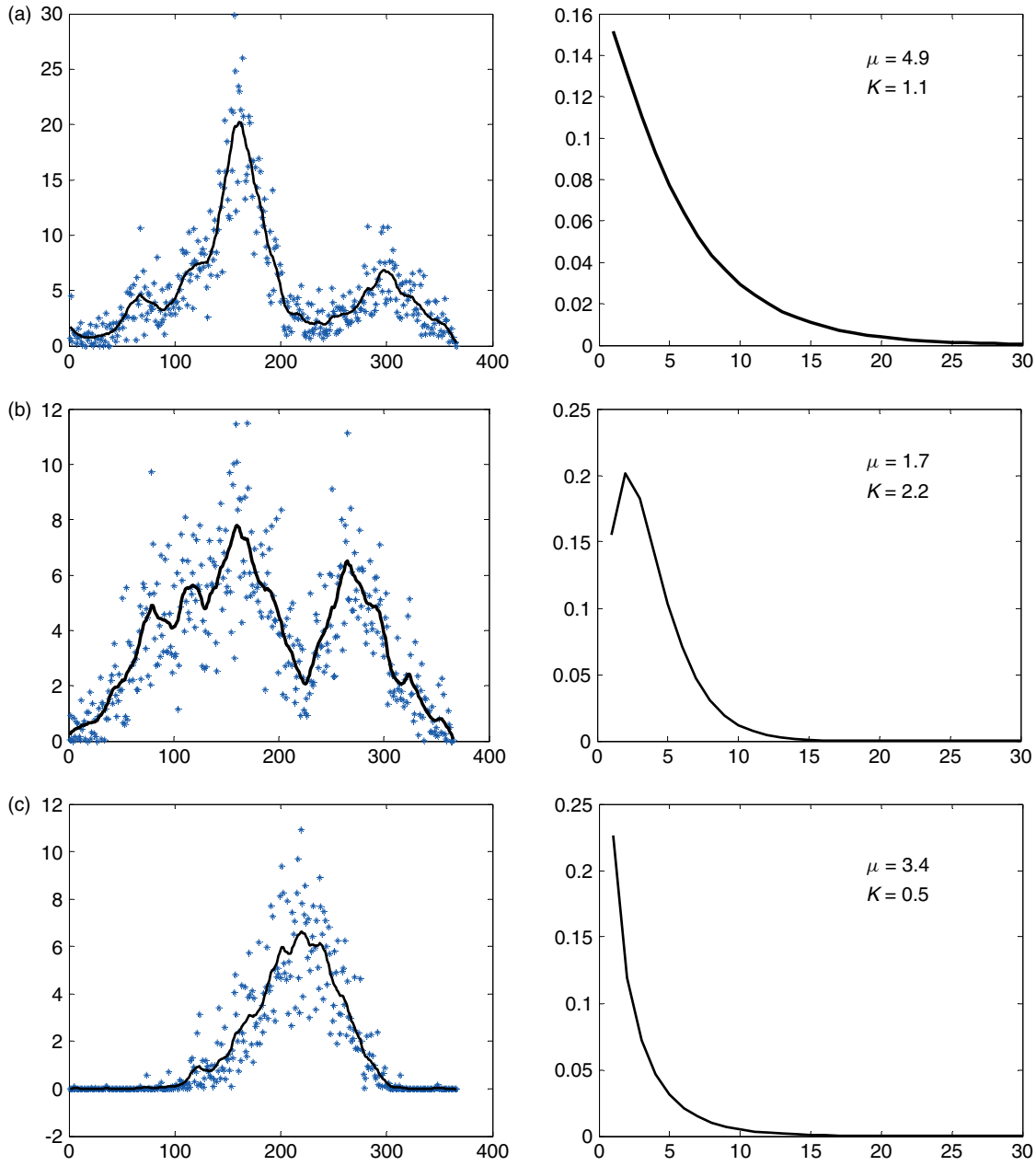

Figure 11. Observed (*) and fitted (−) mean rainfall amount (mm/per day of year) from 1961 to 1999 (left) and its fitted gamma distribution (right) for the stations (a) Axim, (b) Kumasi and (c) Ouahigouya. The location of the stations can be found in Figure 10. This figure is available in colour online at www.interscience.wiley.com/ijoc

mean parameter of the gamma distribution is higher. This leads to a flat probability density function (PDF) compared with other regions of the basin. In the northern part of the basin, represented by station Ouahigouya (Figure 11, bottom), higher values of the mean parameter μ than in the central part, represented by station Kumasi (Figure 11, middle), can be observed. Even though the annual rainfall amounts in the northern region are less than those in the central part, a rainfall event produces averagely more rainfall than in the central part. This is due to the increased number of rainy days in the central part of the Volta Basin. In Kumasi, the rainy season starts earlier than in the coastal zone and the LDS is reduced compared to coastal zone. This is in accordance to results of Laux *et al.* (2008). Additionally, the frequency of rainy days is enhanced and the maximum of the rainfall spectrum is shifted to magnitudes between 2 and 3 mm. Therefore, the shape parameter K exceeds values of 1, which is producing an unimodal shape of the PDF. The differences in the spatial distribution of rainfall events can be explained by the spatial varying influence of the major rain-bearing systems in West Africa (e.g. Fink *et al.*, 2006).

Threshold values of 20 mm/day are used to characterize erosive rainfalls with a potentially high risk of soil loss (e.g. Kowal and Kassam, 1978). Values of 5 mm/day are applied to approximate the daily potential evaporation during the rainy season in West Africa (Garbutt *et al.*,

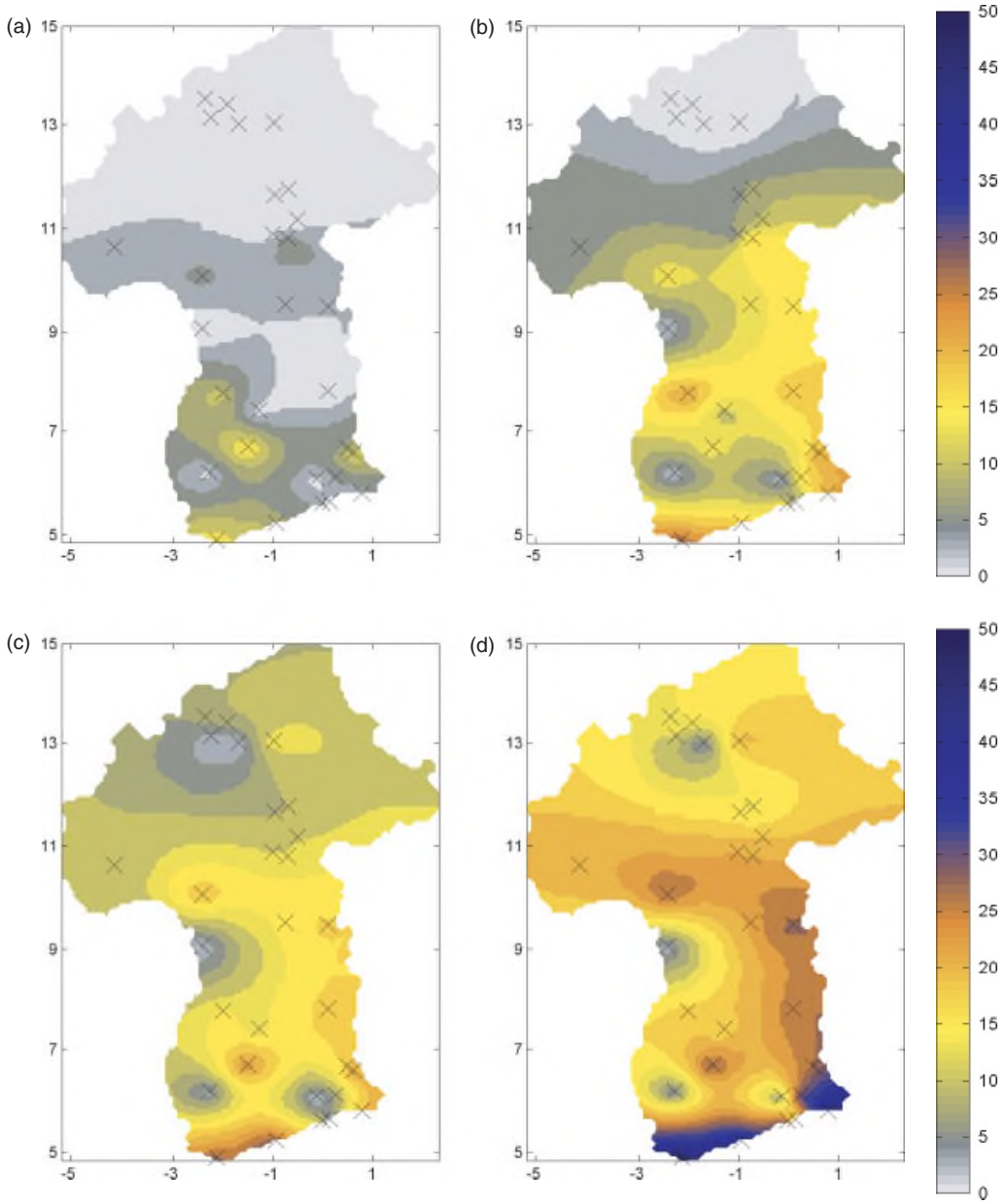

Figure 12. Spatial distribution of rainfall occurrence probabilities (%) exceeding 5 mm/day in the Volta Basin for the month of (a) March, (b) April, (c) May, (d) June, (e) July, (f) August, (g) September and (h) October. External drift kriging, including distance-to-sea information, was applied for spatial interpolation.

1981). The rainfall probabilities exceeding these two thresholds are calculated for each DOY and illustrated in a condensed manner as monthly maps. Figures 12 and 13 display the spatial distribution of occurrence probabilities of rainfall exceeding 5 and 20 mm/day for the months from March to October in the Volta Basin. The probability of rainfall >5 mm/day in June is almost 50% for the coastal area and around 30% for the eastern region. During July, the maximum probability shifts to the central area of Ghana, with low probabilities at the western border of Ghana. In August, high probabilities are reached in Burkina Faso, whereas 0% probability occurs in the southern and western areas of Ghana. In September, the maximum probabilities shift southwards again and are centred in the Volta Basin. In October, the maximum probability is encountered in eastern and western regions of Ghana, while 0% probability is observed for the whole of Burkina Faso. Using the threshold of 20 mm/day, the monthly resolved patterns are almost identicaland only vary in magnitude.

In this paper, a drought is defined as a time period in which one or more consecutive days with 10-day moving-averaged EDI values less than zero occur (Figure 3). The EDI using a 10-day moving-average filter was calculated for five different regions within the Volta Basin from 1961–2001 (Figure 14). The year 1961 served as calibration period. Wet 1960s, dry1970s, severe droughts in the 1980s and wetter 1990s were obtained. These results are in good agreement with many other studies dealing

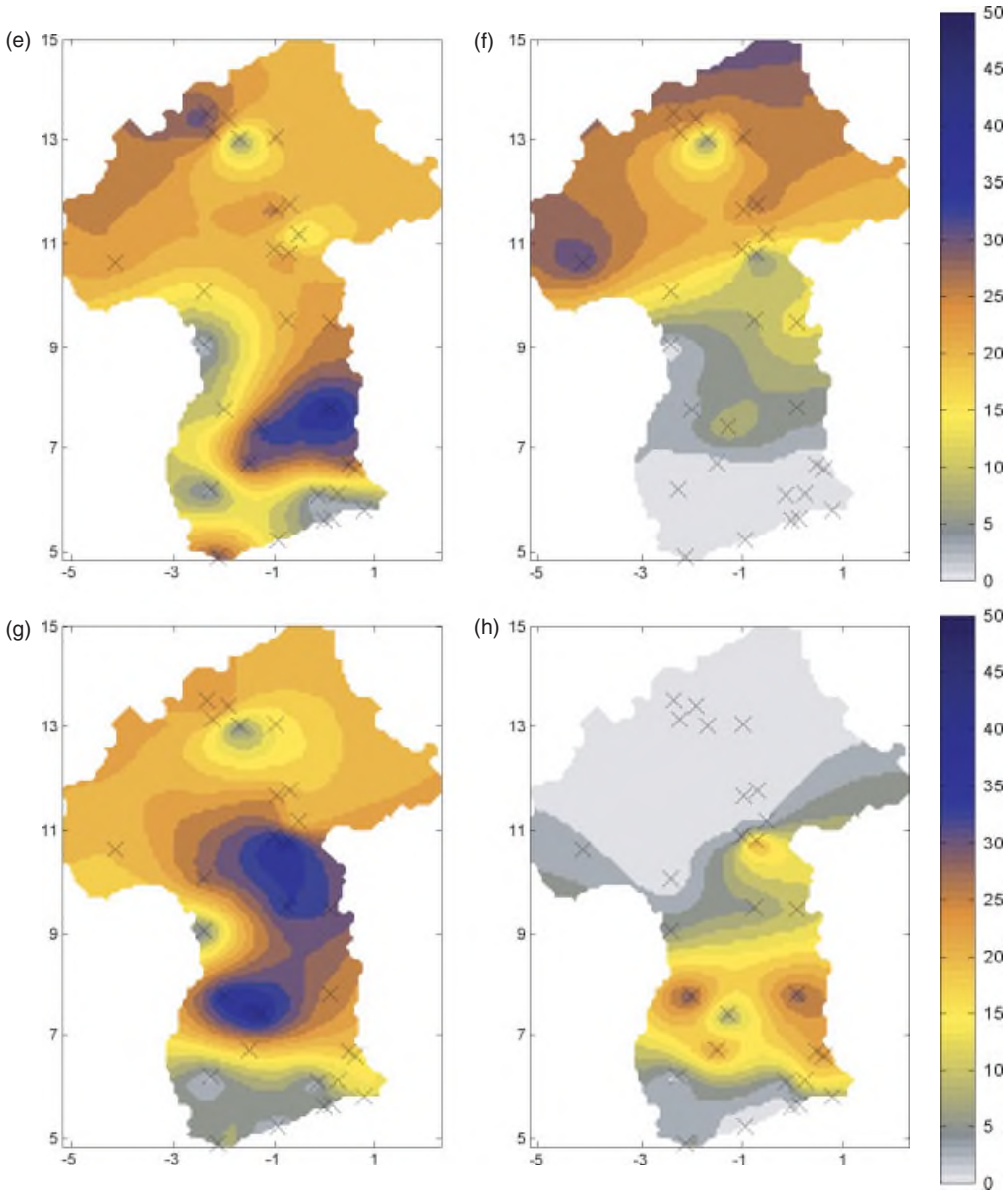

Figure 12. (*Continued*).

with droughts in West Africa (e.g. Lamb and Peppler, 1992; Janicot *et al*., 1996). However, fluctuations in magnitude and duration of droughts can be found between the different regions. In comparison to all the other regions, the coastal region A shows a long-lasting drought period starting in 1998.

From the smoothed EDI values, important drought properties like drought duration, drought intensity and inter-arrival time of droughts were derived. In this context, Figure 15 reflects the influence of the window size of different drought properties in the northernmost region E. The number of drought events drastically decreases from 244 events without using a filter to 47 when applying a 30-day moving-average filter. Applying a 10-day moving-average filter slightly reduces the drought events of the drought intensity classes (Table III) severe and extreme and enhances the moderate class (Figure 16).

Table III. Classification of drought intensity using the effective drought index (EDI).

Normal	0	≥EDI>	−0.7
Moderate	−0.7	≥EDI>	−1.5
Extreme	−1.5	≥EDI>	−2.5
Severe	−2.5	≥EDI>	

The mean values of these drought characteristics of the five different regions obtained by using the 10-day moving-average filter are listed in Table II. Region B reaches the highest mean drought duration (116.4 days) and mean drought intensity values (84.2), calculated as the integral of the EDI values from the onset to the cessation of a drought event. The mean inter-arrival times range from about 144 days (region E) to about 204 days (region B). The drought characteristics of region B

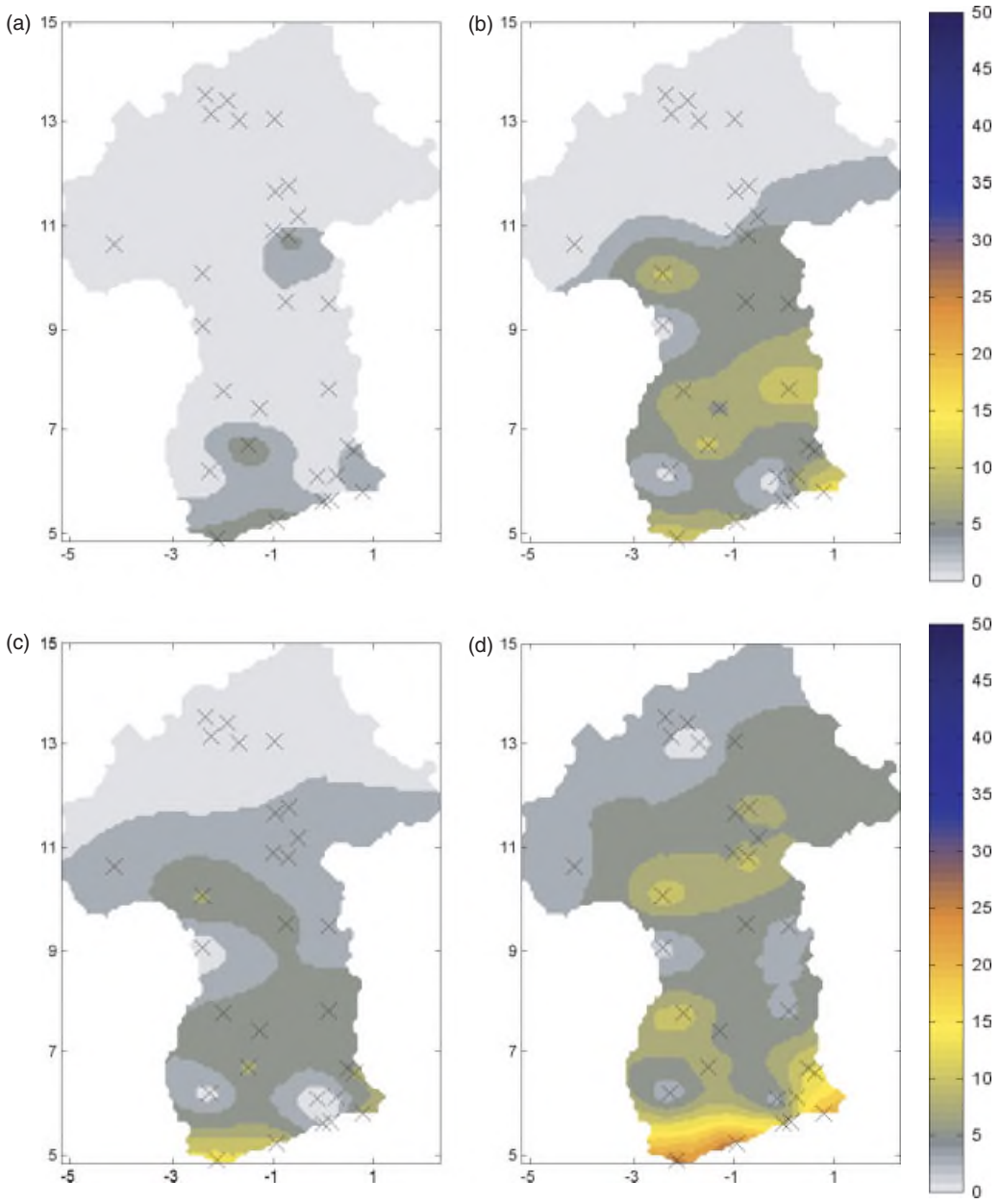

Figure 13. Spatial distribution of rainfall occurrence probabilities (%) exceeding 20 mm/day in the Volta Basin for the month of (a) March, (b) April, (c) May, (d) June, (e) July, (f) August, (g) September and (h) October. External drift kriging, including distance-to-sea information, was applied for spatial interpolation.

show the longest and severest droughts within the Volta Basin.

The most severe drought events occurred within the rainfall regions B and C and started on February 20, 1998 and March 31, 1982, respectively. The bulk of the drought events has drought durations of less than 100 days and drought intensities of less than 100 (cum. EDI values). Strong dependencies between drought duration and drought intensity were found, which vary slightly between the five rainfall regions (Figure 14). Small variations between the Bravais Pearson correlation coefficient and the Spearman rank correlation coefficient (Table IV) indicate a very strong linear dependency between drought duration and drought intensity. Since the dependency structure between the two variables is linear, the Bravais Pearson correlation coefficient also is an appropriate measure. For non-linear dependence, a rank correlation coefficient is more appropriate. These coefficients measure the degree to which large or small values of a variable associate with large or small values of another variable.

Even though the distributions of both variables match a gamma distribution (Figures 17 and 18), a copula approach was chosen in order to model their dependence structure. Alternatively, a bivariate gamma model would also be appropriate in this case. The parameters of the gamma distributions were estimated using the maximum likelihood method (Hahn and Shapiro, 1994).

Figure 19 illustrates the bivariate Clayton–Copula density ratio for rainfall region B by way of example.

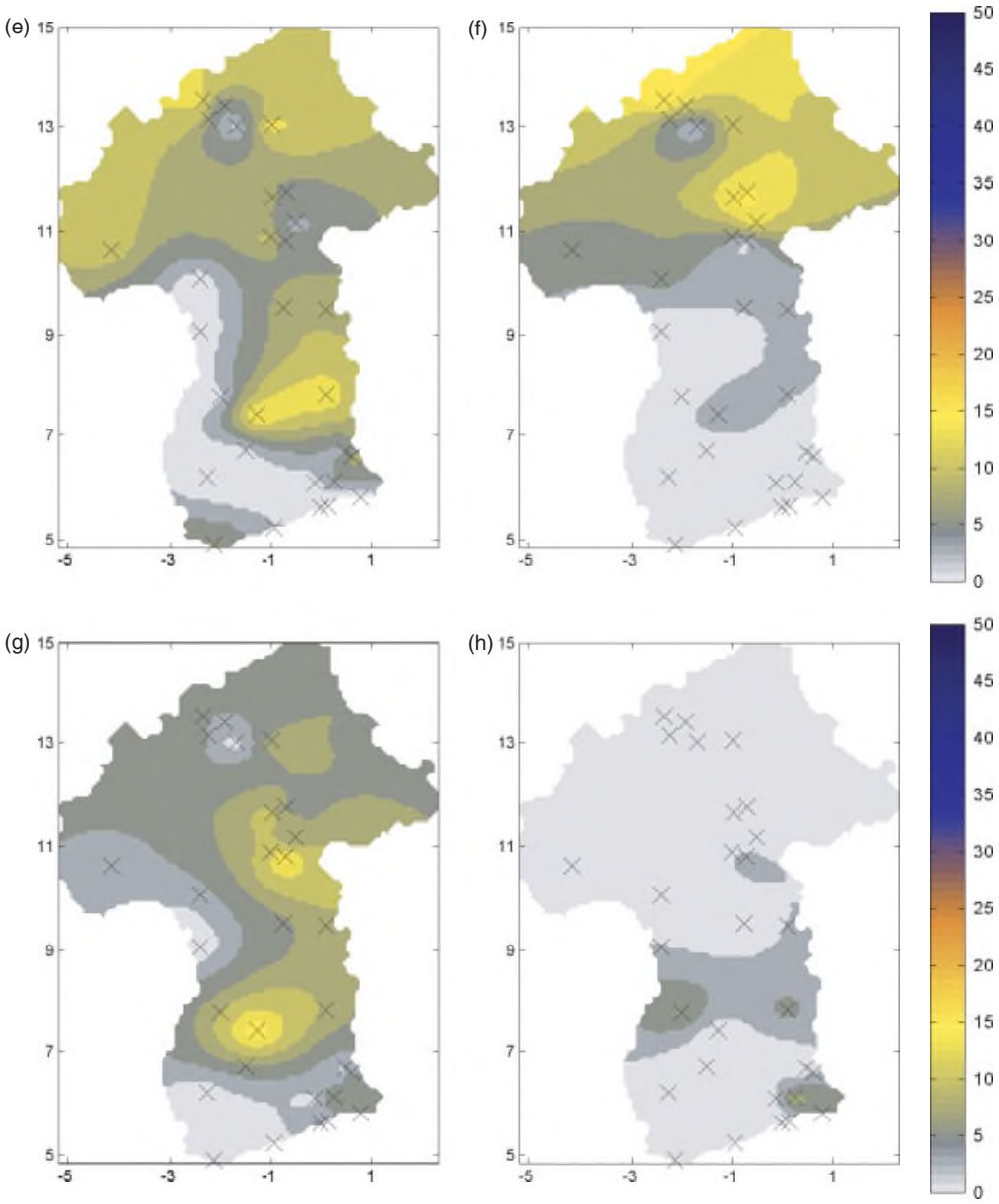

Figure 13. (*Continued*).

The linear structure of the mutual association between drought duration and drought intensity can clearly be seen, varying strongly for the different percentiles. The centre of the density function can be found in the lower percentiles due to the disproportionately high frequency of droughts with short durations and low intensities compared to droughts with high durations and high intensities. The copula parameter Θ was calculated separately for each rainfall region (Table II). The relatively tight parameter range indicates similar shapes of the five different copulas. Figure 20 displays the isolines of bivariate drought duration and drought intensity return periods T_{DS} for the $\wedge$ - case in region A (top) and region E (bottom) using 10-day moving-average EDI values. In both regions, one larger than one-in-1000-year drought occurred. For region A, three larger than one-in-100-year droughts and one larger than one-in-10-year droughts occurred, whereas in region E, no larger than one-in-100-year drought, but four one-in-10-year droughts happened.

The $\vee$ - case, as illustrated in Figure 21, has to be interpreted in a slightly different way: either drought duration or drought intensity can cause one event of a distinct return period, whereas the other parameter is equal to or larger than zero. For region A, for instance, one larger than one-in-1000-year drought occurred, with drought intensity exceeding the values of the $\tau = 1000$ isoline. Within region E, just one larger than one-in-1000-year and one larger than one-in-10-year droughts took place.

5. Summary and outlook

A number of studies dealing with rainfall variability focus on monthly or annual rainfall totals. For agricultural

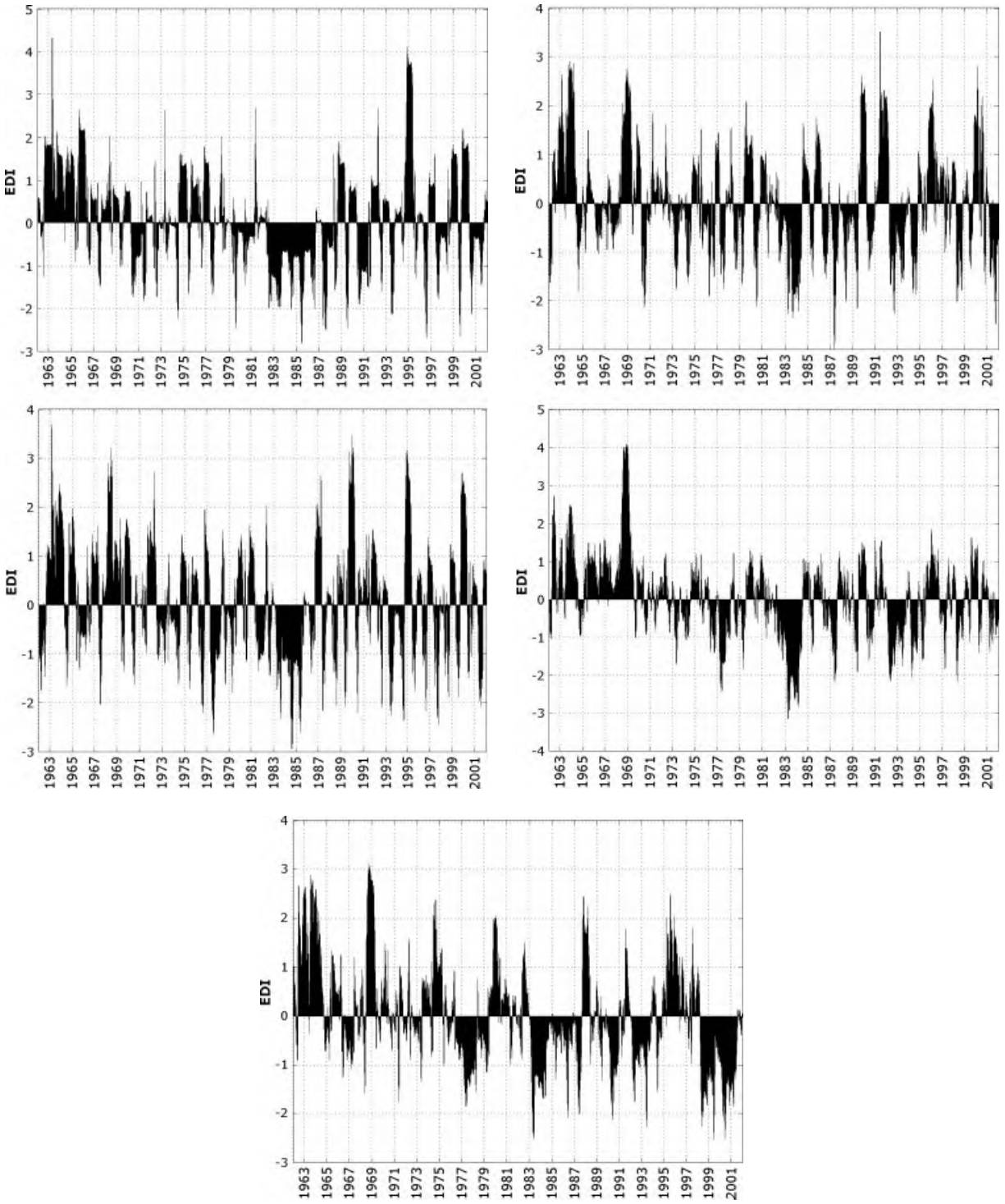

Figure 14. Effective drought index (EDI) for the rainfall regions (e, top), (d), (c), (b) and (a, bottom) using a 10-day moving-average filter. The location of the rainfall regions within the research area can be found in Figure 1.

needs, however, a monthly resolution is too coarse to explain e.g. fluctuations in crop yields, since the distribution of rainfall within the season is the most crucial variable. Crops have specific and varying moisture needs throughout their growth. The identification of crop-specific critical stages during growth and the adaptation in terms of the optimal planting time are the most important factors to minimize crop failure. Therefore, a comprehensive understanding of daily rainfall characteristics is crucial to agricultural production. A major task of the agricultural management in semi-arid to arid environments is to estimate reliably the ORS date and, hence, the optimal planting date. In a former study of Laux *et al.* (2008), a prediction scheme of the ORS in the Volta Basin was proposed. For the predictive mode, no information about the dry spell occurrence for the weeks following planting is available. A major contribution of this paper consists in the derivation of the mean dry spell

Table IV. Sample size and measures of dependence between drought duration and drought intensity (r_{bp} = Bravais Pearson correlation coefficient, ρ_s = Spearman rank correlation coefficient, τ_k = Kendall's Tau) using a 10-day moving-average filter for the EDI values.

Rainfall region	n	r_{bp}	ρ_s	τ_k
A	84	0.96	0.95	0.84
B	71	0.95	0.96	0.84
C	96	0.96	0.99	0.92
D	77	0.98	0.94	0.83
E	99	0.96	0.97	0.85

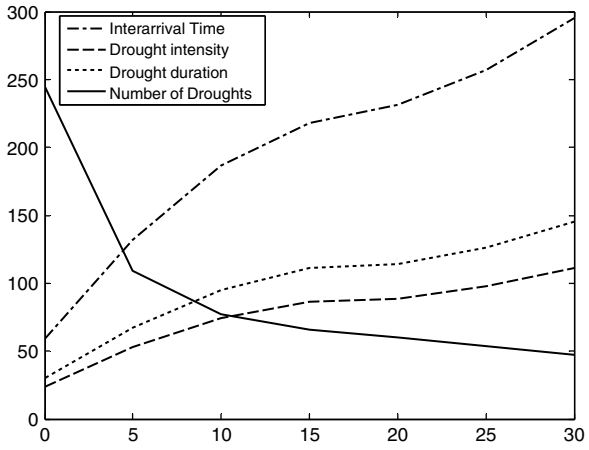

Figure 15. Influence of the moving-average filter with window sizes of 5, 10, 15, 20, 25 and 30 days and of the absence of a moving-average filter (window size = 0) on different mean drought parameters in region E (for the location of region E see, Figure 1).

occurrence probabilities for each DOY and observation site, averaged for the period 1961–1999. Recommendations in the form of optimal time windows for planting dates can be derived, depending on the specific crop type. A map of the 'optimal' planting date, represented by the minimum dry spell probability within the following 30 days for each DOY, is displayed. This information is very useful for farmers or farming managers, since the occurrence of dry spells during the critical stages of plant growth (e. g. establishment, flowering and grain filling) that often decides on the survival or non-survival of the seedlings. On this basis, adapted planting and supplementary irrigation strategies can be derived. In addition, the rainfall probabilities exceeding 5 mm/day (rough estimation of the evaporation during the rainy season in West Africa) and 20 mm/day (potential erosive impacts) are calculated. The probability maps obtained may be used to derive soil protection strategies with a direct spatial linkage. Due to the relatively coarse spatial coverage of the observation network, the presented maps have to be considered with caution.

As droughts are regional in nature, their parameters have to be assessed in a regional context. The Volta Basin was divided into five different regions, which are

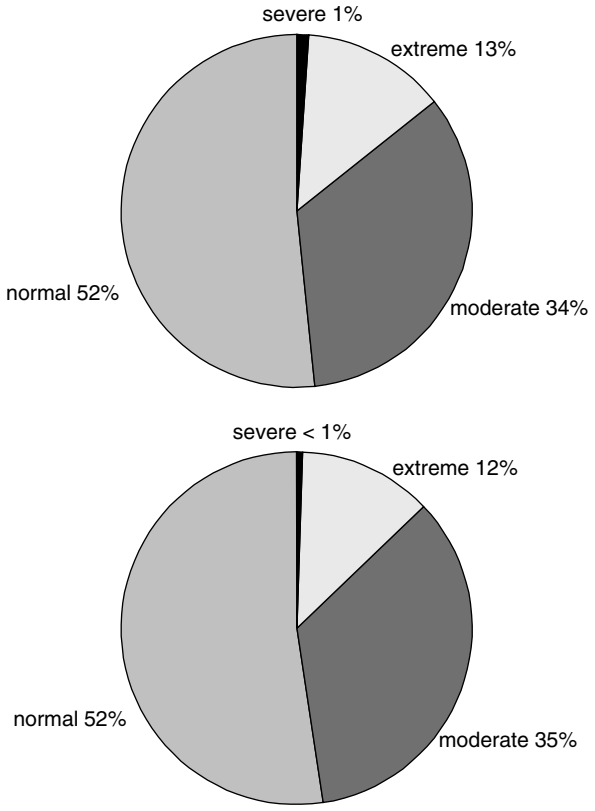

Figure 16. Frequency distribution of the occurrence of the four defined classes (Table III) for rainfall region E. The pie chart at the top shows the distribution of the daily calculated EDI, the one at the bottom shows the distribution using a 10-day moving-average filter.

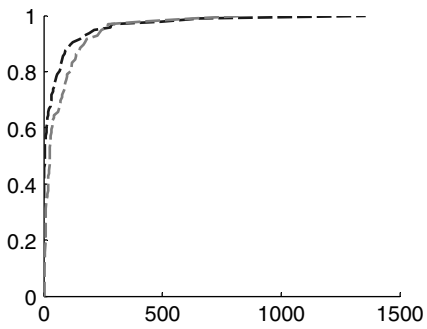

Figure 17. Cumulative density function of drought intensity (black dashed line) and drought duration (grey dashed line) for rainfall region B (for the location of the rainfall regions see, Figure 1).

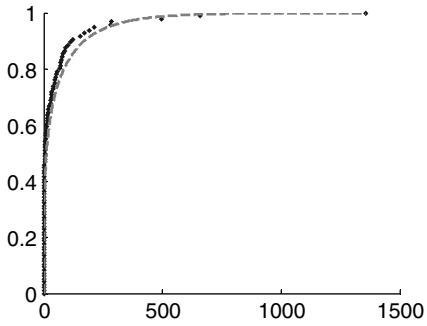

Figure 18. Comparison of the empirical CDF (black diamonds) of drought intensity (cum. EDI) for rainfall region B and its fitted CDF (grey dashed line).

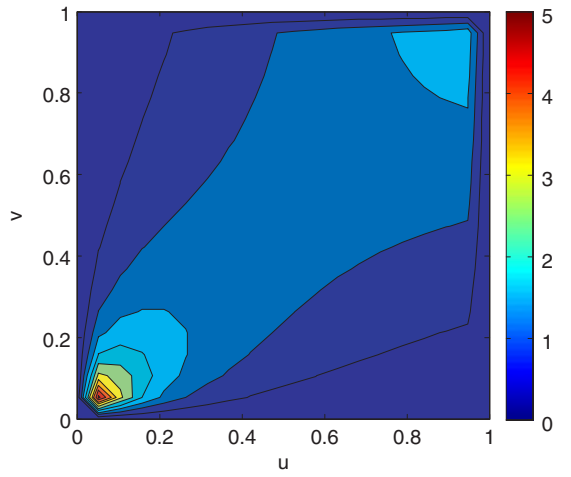

Figure 19. Contour plot of the bivariate Clayton copula density for $\Theta = 7.29$, corresponding to rainfall region B (for the location of the rainfall regions, see Figure 1), u is the transformed drought duration and v is the transformed drought intensity. This figure is available in colour online at www.interscience.wiley.com/ijoc

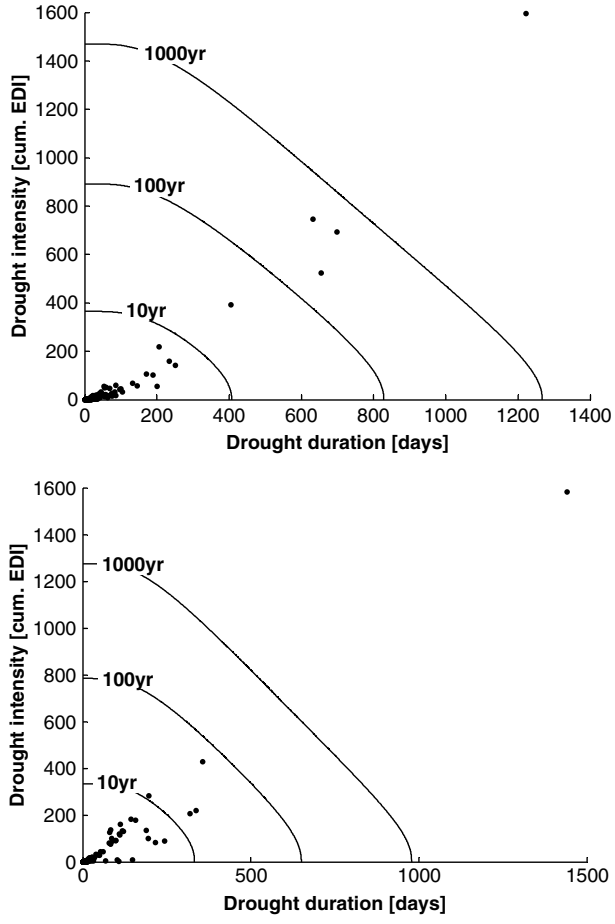

Figure 20. Isolines of return periods T_{DS} accounting for drought duration and drought intensity exceeding a specific value ($\wedge$ - case) in region A (top) and region E (bottom). The location of the rainfall regions within the research are can be found in Figure 1. A 10-day moving-average filter for the EDI values is used. The dots represent the single drought events.

arranged zonally. The EDI was used for quantitative drought definition in terms of drought duration and drought intensity. A quantitative approach allows for

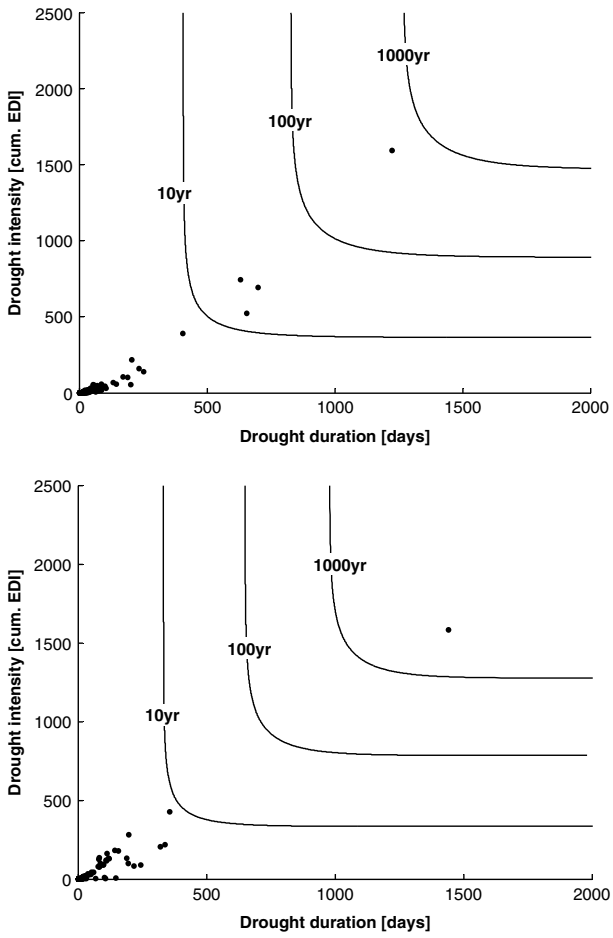

Figure 21. Isolines of return periods T_{DS} accounting for drought duration or drought intensity exceeding a specific value ($\vee$ - case) in region A (top) and region E (bottom). The location of the rainfall regions within the research are can be found in Figure 1. A 10-day moving-average filter for the EDI values is used. The dots represent the single drought events.

the establishment of an operational drought monitoring system for the Volta Basin.

A copula approach was used to simultaneously model the dependence between drought duration and drought intensity. Regional return periods of droughts were derived. As droughts cannot be avoided, adaptation strategies must be derived for agriculture. On the basis of the regional return periods derived, highly drought-resistant crop varieties must be planted in regions with most frequently recurring droughts. Unresistant crop varieties should be displaced to other regions.

The flexible copula approach allows for the integration of other drought-relevant parameters and is therefore preferred to e.g. the bivariate gamma distribution model. Potential input parameters should capture the variability of rainfall and thus contributing to droughty or wet conditions within the Volta Basin, e.g. the ENSO (Adiku and Stone, 1995). The Clayton copula has proved suitable for various hydrologic needs (e.g. Favre *et al.*, 2004; Shiau *et al.*, 2007). However, the question as to which copula model fits best to the empirical data still remains to be answered and is far beyond the scope of the present work.

Acknowledgements

This work was funded by the German Ministry of Education and Research (BMBF) within the GLOWA Volta project. The financial support is gratefully acknowledged.

References

Adiku SGK, Stone RC. 1995. Using the Southern oscillation index for improving rainfall prediction and agricultural water management in Ghana. *Agricultural Water Management* **29**: 85–100.

Ahmed S, de Marsily G. 1987. Comparison of geostatistical methods for estimating transmissivity using data on transmissivity and specific capacity. *Water Resources Research* **23**: 1717–1737.

Ali A, Lebel T, Amani A. 2003. Invariance in the spatial structure of Sahelian rain fields at climatological scales. *Journal of Hydrometeorology* **4**: 996–1011.

Ati OF, Stigter CJ, Oladipo EO. 2002. A comparison of methods to determine the onset of the growing season in Northern Nigeria. *International Journal of Climatology* **22**: 731–742.

Buishand TA. 1977. In *Stochastic Modelling of Daily Rainfall Sequences*, Veenman H, Zonen BV (eds). Wageningen: Netherlands; 211.

Cancelliere A, Salas JD. 2004. Drought length properties for periodic-stochastic hydrologic data. *Water Resources Research* **40**: W02503.

Chatterjea K. 1998. The impact of tropical rainstorms on sediment and runoff generation from bare and grass-covered surfaces: a plot study from Singapore. *Land Degradation & Development* **9**(2): 143–157.

Chin EH. 1977. Modelling daily precipitation process with Markov chain. *Water Resources Research* **13**: 949–956.

D'Amato N, Lebel T. 1998. On the characteristics of the rainfall events in the Sahel with a view to the analysis of climatic variability. *International Journal of Climatology* **18**: 955–974.

Dracup JA, Lee KS, Paulson EG. 1980a. On the definition of droughts. *Water Resources Research* **16**: 297–302.

Dracup JA, Lee KS, Paulson EG. 1980b. On the statistical characteristics of drought events. *Water Resources Research* **16**: 289–296.

Dunn PK, White N. 2005. Power-variance models for modelling rainfall. In *Statistical Solution to Modern Problems: Proceedings of the 20th International Workshop on Statistical Modelling*, Sydney, 11–15 July 2005, 149–156.

Favre A-C, El Adlouni IS, Perreault L, Thiémonge N, Bobée B. 2004. Multivariate hydrological frequency analysis using copulas. *Water Resources Research* **40W01101**: 1–12.

Fink AH, Vincent DG, Ermert V. 2006. Rainfall types in the West African Sudanian Zone during the Summer Monsoon 2002. *Monthly Weather Review* **134**(8): 2143–2164.

Garbutt DJ, Stern RD, Dennett MD, Elston J. 1981. A comparison of the rainfall climate of eleven places in West Africa using a two-part model for daily rainfall. *Meteorology and Atmospheric Physics* **29**: 137–155.

Hahn GJ, Shapiro SS. 1994. *Statistical Models in Engineering*. John Wiley and Sons: New York; 88.

Hisdal H, Tallaksen LM. 2003. Estimation of regional meteorological and hydrological drought characteristics: a case study for Denmark. *Journal of Hydrology* **281**: 230–247.

Ingram KT, Roncoli MC, Kirshen PH. 2002. Opportunities and constraints for farmers of West Africa to use seasonal precipitation forecasts with Burkina Faso as a case study. *Agricultural Systems* **74**: 331–349.

Janicot S, Moron V, Fontaine B. 1996. Sahel droughts and ENSO dynamics. *Geophysical Research Letters* **23**: 515–518.

Jimoh OD, Webster P. 1999. Stochastic modelling of daily rainfall in Nigeria: inter-annual variation of model parameters. *Journal of Hydrology* **222**: 1–17.

Kowal JA, Kassam AH. 1978. *Agricultural Ecology of Savannah – a Study of West Africa*. Oxford University Press: UK.

Kunstmann H, Jung G. 2007. Influence of soil moisture and land use change on precipitation in West Africa. *International Journal of River Management* **5**(1): 9–16.

Lamb PJ, Peppler RA. 1992. Further case studies of tropical Atlantic surface atmospheric and oceanic patterns associated with sub-Saharan drought. *Journal of Climate* **5**: 476–488.

Laux P, Kunstmann H, Bárdossy A. 2007. Linking the West African monsoon's onset with atmospheric circulation patterns. Quantification and Reduction of Predictive Uncertainty for Sustainable Water Resource Management. *IAHS Publ.* **313**: 40–50.

Laux P, Kunstmann H, Bárdossy A. 2008. Predicting the regional onset of the rainy season in West Africa. *International Journal of Climatology* **28**(3): 329–342.

Le Barbé L, Lebel T. 1997. Rainfall climatology of the Hapex Sahel region during the years 1950–1990. *Journal of Hydrology* **188–189**: 43–73.

Le Barbé L, Lebel T, Tapsoba D. 2002. Rainfall variability in West Africa during the years 1950–1990. *Journal of Climate* **15**: 187–202.

L'Hôte Y, Mahé G, Somé B, Triboulet JP. 2002. Analysis of a Sahelian annual rainfall index from 1896 to 2000; the drought continues. *Hydrological Sciences Journal* **47**(4): 563–572.

Mahé G, L'Hôte Y, Olivry J-C, Wotling G. 2001. Trends and discontinuities in regional rainfall of West and Central Africa: 1951–1989. *Hydrological Sciences Journal* **46**(2): 211–226.

Mathier L, Perreault L, Bobe B, Ashkar F. 1992. The use of geometric and gamma-related distributions for frequency analysis of water deficit. *Hydrology and Hydraulics* **6**: 239–254.

Morid S, Smakhtin V, Moghaddasi M. 2006. Comparison of seven meteorological indices for drought monitoring in Iran. *International Journal of Climatology* **26**(7): 971–985.

Neumann R, Jung G, Laux P, Kunstmann H. 2007. Climate trends of temperature, precipitation and river discharge in the Volta Basin of West Africa. *International Journal of River Management* **5**(1): 17–30.

Omotosho JB, Balogun AA, Ogunjobi JK. 2000. Predicting monthly and seasonal rainfall, onset and cessation of the rainy season in West Africa using only surface data. *International Journal of Climatology* **20**: 865–880.

ORSTOM. 1996. Afrique de'l Ouest et Centrale Précipitations Moyennes Annuelles (Période 1951–1989), Laboratoire d'Hydrologie, B.P. 5045, 34032 Montepellier, Cedex, France.

Pielke RA Sr, Avissar R, Raupach M, Dolman H, Zeng X, Denning S. 1998. Interactions between the atmosphere and terrestrial ecosystems: Influence on weather and climate. *Global Change Biology* **4**: 101–115.

Salvadori G. 2004. Bivariate return periods via 2-Copulas. *Statistical Methodology* **1**: 129–144.

Shapiro BI, Winslow M, Traoré PS, Balaji V, Cooper P, Rao KPC, Wani S, Koala S. 2007. CGIAR efforts, capacities and partner opportunities. In *Climate Application and Agriculture*, Sivakumar MVK, Hansen, J (eds). Springer: Berlin Heidelberg.

Shiau J-T, Feng S, Nadarajah S. 2007. Assessment of hydrological droughts for the Yellow River, China, using copulas. *Hydrological Processes* **21**(16): 2157–2163.

Sivakumar MVK. 1988. Predicting rainy season potential from the onset of rains in Southern Sahelian and Sudanian climatic zones of West Africa. *Agricultural and Forest Meteorology* **42**: 295–305.

Sivakumar MVK. 1992. Climate change and implications for agriculture in Niger. *Climatic Change* **20**(4): 297–312.

Sklar A. 1959. *Fonctions de Répartition à n Dimensions et leurs Marges*. Publications de l'Institut de Statistique de L'Université de Paris: France; **8**: 229–231.

Smakhtin VU, Hughes DA. 2007. Automated estimation and analyses of meteorological drought characteristics from monthly rainfall data. *Environmental Modelling & Software* **22**(6): 880–890, ISSN 1364–8152.

Stern RD, Dennett MD, Garbutt DJ. 1981. The start of the rains in West Africa. *Journal of Climatology* **1**: 59–68.

Stern RD, Coe R. 1982. The use of rainfall models in agricultural planning. *Agricultural Meteorology* **26**: 35–50.

Stewart JI. 1991. Principles and performance of response farming. In *Climatic Risk in Crop Production. Models and Management for the Semi-Arid Tropics and Sub-Tropics*, Ford W, Muchow RC, Bellamy ZA (eds). CAB International: Wallingford.

Sultan B, Baron C, Dingkuhn M, Sarr B, Janicot S. 2005. Agricultural impacts of large-scale variability of the West African Monsoon. *Agricultural and Forest Meteorology* **128**: 93–110.

Tallaksen LM, Madsen H, Clausen B. 1997. On the definition and modelling of streamflow drought duration and deficit volume. *Hydrological Sciences Journal-Journal Des Sciences Hydrologiques* **42**(1): 15–33.

Usman MT, Reason CJJ. 2004. Dry spell frequency and their variability over southern Africa. *Climate Research* **26**: 199–211.

Walter MW. 1967. Length of the rainy season in Nigeria. *Nigerian Geographical Journal* **10**: 123–128.

Wilhite DA, Glantz MH. 1985. Understanding the drought phenomenon: The role of definitions. *Water International* **10**(3): 111–120.